



# Adsorption removal of phosphate in industrial wastewater by using metal-loaded skin split waste

Xin Huang, Xuepin Liao\*, Bi Shi\*

National Engineering Laboratory for Clean Technology of Leather Manufacture, Sichuan University, Chengdu, 610065, PR China

## ARTICLE INFO

### Article history:

Received 18 August 2008  
Received in revised form 5 December 2008  
Accepted 6 December 2008  
Available online 11 December 2008

### Keywords:

Phosphate removal  
Adsorption  
Solid waste  
Skin collagen  
Metal-loaded adsorbent

## ABSTRACT

Leather industry inevitably generates a large amount of skin split waste (SSW) due to the necessary operation of splitting in leather making process. In this study, two adsorbents, SSW-Fe and SSW-Al, were prepared by loading Fe(III) and Al(III) onto SSW, and their adsorption behaviors to phosphate in industrial wastewater were investigated through batch and column adsorption experiments. The macro-adsorption kinetics data obtained from batch experiments were well fitted by the pseudo-second-order rate model and the adsorption isotherms can be well described by the Langmuir equation. The adsorption behaviors of the columns can be well described by Yoon and Nelson model and the time at breakthrough point can be accurately predicted by this model. It was found that the metal-loaded adsorbents prepared by using SSW as supporting matrix can effectively remove phosphate from industrial wastewater. The leakage of metal ions during adsorption process is neglectable. These results indicate that the metal-loaded SSW adsorbents have a good future in practical application for the removal of phosphate from industrial wastewater.

Crown Copyright © 2008 Published by Elsevier B.V. All rights reserved.

## 1. Introduction

Excessive phosphate in water is one of the main factors leading to eutrophication and deterioration of water bodies [1]. The eutrophication would happen when the concentration of phosphate in water bodies is higher than 0.02 mg/L [2]. The phosphate-containing industrial wastewater discharged into lakes, rivers and other natural waters is one of the major sources of excessive phosphate in water bodies. Therefore, from the perspective of environmental protection, it is necessary to remove phosphate from industrial wastewater.

The phosphate in industrial wastewater can be removed by physicochemical and biological methods. Chemical precipitation with alum, lime and iron salts is often used for the removal of phosphate from wastewater. However, this method is subjected to costs and the problem of sludge handling. Moreover, chemical precipitation is less effective when the concentration of phosphate is in trace level [3]. The biological removal of phosphate from wastewater has been developed since 1950s, but only 10–30% of phosphate can be removed by this technology [4]. Indeed, biological treatment can hardly reduce the concentration of phosphate to the discharge limit of 0.5 mg/L [5] due to the fact that phosphate is one of the necessary elements for metabolism of microorganisms, and some

microorganisms cannot live in the absence of phosphate. Adsorption is comparatively more useful and economical approach for the removal of phosphate from industrial wastewater, particularly for the treatment of phosphate-containing wastewater with low concentration [6].

Some industrial by-products have been used as adsorbents for the removal of phosphate from wastewater. For example, it was reported that blast furnace slag from steel industry [7], dewatered alum sludge from wastewater treatment plants [8] and fly ash from power station [9] can be used for the removal of phosphate. The advantage of using these by-products as adsorbents is cost effectiveness in addition to the alleviation of environmental pressure caused by industrial by-products. However, these by-products are hardly used in practical application due to their low and unstable adsorption capacities to phosphate [10].

Skin split waste (SSW) is one of the major solid wastes produced in leather industry. In China, approximately 0.51 million ton of SSW are produced from tanneries every year [11,12]. The solid wastes in tanneries are usually land filled or burnt, which might cause second environmental pollution. Therefore, great efforts have been made to explore the approaches of utilizing these wastes. It has been reported that SSW can be used as raw material to produce feed additives [13] and hydrolyzed products such as gelatin [14]. However, these utilizations of SSW have been prohibited in some countries due to the potential negative effect of the products to domestic animals and human beings.

\* Corresponding author. Tel.: +86 28 85405508; fax: +86 28 85400356.  
E-mail address: [xpliao@scu.edu.cn](mailto:xpliao@scu.edu.cn) (X. Liao).

**Table 1**  
Chemical components in the wastewater from an automobile factory (pH 6.50–7.20).

| Components           | COD   | BOD <sub>5</sub> | Phosphate | Lead  | Arsenic | Cadmium | Hydrargyrum |
|----------------------|-------|------------------|-----------|-------|---------|---------|-------------|
| Concentration (mg/L) | 50–60 | 60–70            | 1.7–1.8   | 0.068 | 0.008   | 0.050   | 0.001       |

The main component of SSW is collagen fiber, which is capable of reacting with many metal ions such as Fe(III), Al(III), Zr(IV) etc. [15]. It is well known that metal oxides or metal hydroxides are the functional components of many adsorbents used for adsorption of phosphate [16]. Our previous investigation also proved that the metal ions loaded onto collagen fiber can effectively remove phosphate from aqueous solution [17]. Therefore, it is possible to develop metal-loaded adsorbent suitable for the adsorption of phosphate by using SSW as supporting material. In this study, two adsorbents were prepared by loading Fe(III) or Al(III) onto SSW and their fundamental adsorption behaviors to phosphate in aqueous solution and in industrial wastewater were investigated.

## 2. Materials and methods

### 2.1. Materials

The pigskin split wastes were collected from a local tannery. The industrial wastewater used in experiments was taken from an automobile factory, and its main components determined are summarized in Table 1. Other chemicals used in experiments were all analytical reagents.

### 2.2. Preparation and characterization of adsorbents

15.0 g SSW were fully washed with distilled water, and then soaked in 400 mL water of pH 1.70–2.00 adjusted by HCOOH and H<sub>2</sub>SO<sub>4</sub> solutions. After being stirred at room temperature for 2 h, 0.1 mol Fe(III) or Al(III) was added and the reaction was undertaken with constant stirring at 30 °C for 6 h. Then, a proper amount of NaHCO<sub>3</sub> solution (15%, w/w) was gradually added within 2 h in order to increase the pH of the solution to 4.00–4.20, and the reaction was continued at 45 °C for another 4 h. When the reaction was completed, the product was collected by filtration, washed with distilled water, dried in vacuum at 50 °C for 12 h, and ground into particle of 0.5–1.0 mm. Then the Fe(III)- and Al(III)-loaded adsorbents on the basis of SSW were obtained (denoted as SSW-Fe and SSW-Al, respectively).

The concentration of Fe(III) or Al(III) in the residual solution after reaction was determined by means of Inductively Coupled Plasma-atomic Emission Spectroscopy (ICP-AES, PerkinElmer Optima 2100DV, German), and the content of metal ion loaded onto SSW was determined by mass balance calculation. The heat denaturation temperatures of SSW-Fe and SSW-Al were determined by differential scanning calorimetry (DSC, PC 200DSC, NETZSH Company, Germany). The specific areas of SSW-Fe and SSW-Al were determined by surface area and porosity analyzer (TriStar 3000, Micromeritics, U.S.) and other physical properties of the adsorbents were tested by common methods. The physical properties of SSW-Fe and SSW-Al were summarized in Table 2.

**Table 2**  
Physical properties of SSW-Fe and SSW-Al.

| Parameters                                       | SSW-Al    | SSW-Fe    |
|--|-----------|-----------|
| Metal ion content (mmol/g)                       | 6.00      | 6.02      |
| Specific area (m <sup>2</sup> /g)                | 4.68      | 5.23      |
| Denaturation temperature (K)                     | 343–348   | 358–360   |
| Bulk density (in dry state) (g/cm <sup>3</sup> ) | 0.28–0.31 | 0.16–0.17 |
| Water absorptivity (g/g)                         | 4.20–4.38 | 1.60–1.90 |

### 2.3. Adsorption capacities of SSW-Fe and SSW-Al to phosphate in aqueous solutions

0.1 g adsorbent was suspended in 100 mL of phosphorus solution with pH 7.0 adjusted by using 0.1 M NaOH solution. The initial concentration of phosphate was varied from 0.5 to 3.0 mmol/L. The adsorption was conducted with constant shaking at 303 K for 24 h. The concentration of phosphate in residual solution was determined by ICP-AES, and the adsorption capacity was obtained by mass balance calculation.

### 2.4. Batch adsorption kinetics of phosphate in industrial wastewater

0.1 g adsorbent was suspended in 100 mL of industrial wastewater (1.7 mg P/L). The adsorption was conducted by constant shaking at 303 K and the concentration of phosphate in solution was analyzed at a regular interval by ICP-AES.

### 2.5. Column adsorption study of phosphate in industrial wastewater

The adsorbent was soaked in distilled water for 12 h, and then was filled into a column of diameter 1.10 cm and height 22.00 cm. The column was equilibrated with distilled water for 4 h to ensure that the column was fully wet and all the air between and within the adsorbent was expelled. In addition, the liquid level on column was kept 0.5–0.8 cm higher than the top of adsorbent during adsorption process. The phosphate-containing industrial wastewater (1.7 mg P/L) was pumped into the columns with a constant flow rate of 40 mL/h. The effluent was collected by an automatic collector and the concentration of phosphate in the effluent was analyzed by ICP-AES. The concentrations of Fe(III) and Al(III) in effluent were also detected by ICP-AES. The schematic diagram of column adsorption system is shown in Fig. 1.

## 3. Results and discussion

### 3.1. Adsorption capacity of metal-loaded adsorbents to phosphate in aqueous solutions

The adsorption isotherms of SSW-Fe and SSW-Al to phosphate are shown in Fig. 2. It can be observed that the adsorption capacity

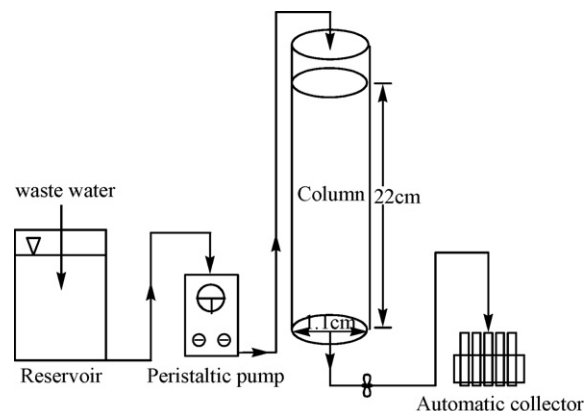


**Fig. 1.** Schematic diagram of column adsorption system.

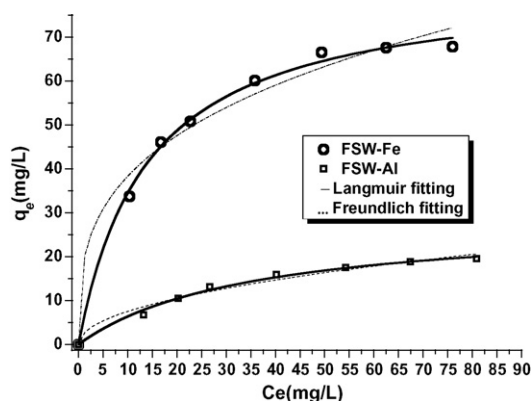


Fig. 2. Isothermal fittings of phosphate adsorbed on FSW-Fe and FSW-Al (303 K, 24 h, averages of three separate measurements).

of SSW-Fe is higher than that of SSW-Al at the same equilibrium concentration of phosphate, probably due to the stronger chelating ability of SSW-Fe with anionic species of phosphate. The adsorption capacity of SSW-Fe to phosphate was about 68.00 mg/g when the initial concentration of phosphate was 93.00 mg/L, while the adsorption capacity of SSW-Al was only 19.50 mg/g in the same conditions. The control experiments showed that raw SSW almost has no adsorption ability to phosphate, which indicates that the metal ions loaded on SSW are the main active positions for the adsorption. It was reported that active carbon almost has no adsorption ability to phosphate [18], and the adsorption capacity of active alumina which is often used for the adsorption of phosphate was in the range of 10.0–30.0 mg/g under the optimal conditions [19,20]. Therefore, the adsorption capacity of SSW-Fe to phosphate is much higher than that of other commonly used adsorbents. The adsorption isotherms were further analyzed by the Langmuir model (1) [21] and Freundlich model (2) [22]:

$$q_e = \frac{bq_{\max}c_e}{1 + bc_e} \quad (1)$$

$$\frac{t}{q_t} = \frac{1}{kq_e^2} + \frac{1}{q_e}t \quad (2)$$

where  $q_e$  and  $c_e$  are the amounts of phosphate adsorbed (mg/g) and the concentration of phosphate in the bulk solution (mg/L) at equilibrium, respectively,  $b$  is the Langmuir parameter relating to the strength of adsorption ( $\text{mg}^{-1}$ ),  $q_{\max}$  is the maximum adsorption capacity (mg/g),  $k$  and  $n$  are the Freundlich constants. The parameters of the Langmuir and Freundlich fittings are summarized in Table 3. It can be observed that the Langmuir equation gives more satisfactory fitting to the adsorption isotherms of phosphate on SSW-Fe and SSW-Al with correlation coefficient  $R^2$  higher than 0.95. The theoretical adsorption capacities of SSW-Fe and SSW-Al to phosphate calculated by the Langmuir equation are 72.00 and 21.65 mg P/g, respectively, which are very close to those determined by experiments.

Table 3

Langmuir and Freundlich isothermal parameters for the adsorption of phosphate on SSW-Fe and SSW-Al.

|        | $q_{e,\text{exp}}$ (mg/g) | Langmuir          |       |       | Freundlich |       |       |
|--------|---------------------------|-------------------|-------|-------|------------|-------|-------|
|        |                           | $q_{\max}$ (mg/g) | $b$   | $R^2$ | $n$        | $k$   | $R^2$ |
| SSW-Al | 19.50                     | 21.65             | 5.74  | 0.95  | 3.2        | 18.66 | 0.95  |
| SSW-Fe | 67.80                     | 72.00             | 11.43 | 0.97  | 2.7        | 2.46  | 0.95  |

$q_{e,\text{exp}} = q_{e,\text{experiments}}$

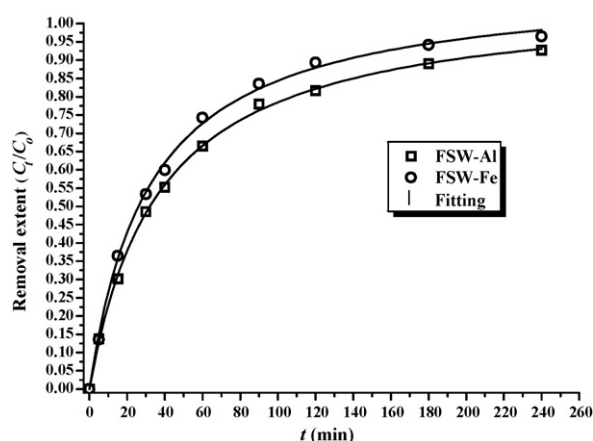


Fig. 3. Adsorption kinetics of phosphate on SSW-Fe and SSW-Al (303 K, 0.1 g adsorbent).

### 3.2. Batch adsorption kinetics of phosphate in industrial wastewater

The batch adsorption kinetics of SSW-Fe and SSW-Al to phosphate in industrial wastewater are presented in Fig. 3. It can be observed that about 80% of phosphate is removed after 2 h of the adsorption, implying that the content of phosphate in the solution is below the discharge limit of 0.5 mg/L. In addition, the adsorption rates of phosphate on SSW-Fe and SSW-Al are very fast as compared with other porous adsorbents [23]. However, as it can be seen in Table 2, the specific areas of SSW-Fe and SSW-Al are much smaller than those of other porous adsorbents. In fact, SSW-Fe and SSW-Al are in fibrous state, which suggests that the adsorption of phosphate should take place at the outer surface of SSW-Fe and SSW-Al and the diffusion resistance of mass transfer can be neglected.

The macro-adsorption kinetics data were further analyzed by using the kinetic model of pseudo-second-order Eq. (3) [24]:

$$\frac{t}{q_t} = \frac{1}{kq_e^2} + \frac{1}{q_e}t \quad (3)$$

where  $q_e$  and  $q_t$  are the amount of phosphate adsorbed on adsorbent (mg/g) at equilibrium and at time  $t$  (min), respectively, and  $k$  is the constant of pseudo-second-order rate (mg/g min). Based on the experimental data of  $q_t$  and  $t$ , the equilibrium adsorption capacity ( $q_e$ ) and the pseudo-second-order rate constant ( $k$ ) can be determined from the slope and intercept of a plot of  $t/q_t$  versus  $t$ . It was found that the pseudo-second-order model gives a satisfactory fit to all of the experimental data. The fitting parameters of the pseudo-second-order model are summarized in Table 4.

### 3.3. Column adsorption studies

The breakthrough curves of phosphate in industrial wastewater on SSW-Fe and SSW-Al adsorption columns are presented in Fig. 4a and b. The breakthrough point of SSW-Fe column is about 18,000 mL, while it is only about 260 mL for SSW-Al column. This is consistent with their adsorption capacity, as shown in Section 3.1.

Table 4

The pseudo-second-order model parameters of phosphate adsorption kinetics on SSW-Fe and SSW-Al (pH 7.0, initial concentration of phosphate = 1.7 mg/L).

| Adsorbent | $k \times 10^2$ (mg/g min) | $q_{e,\text{exp}}$ (mg P/g) | $R^2$  |
|-----------|----------------------------|-----------------------------|--------|
| SSW-Al    | 1.782                      | 1.750                       | 0.9993 |
| SSW-Fe    | 1.883                      | 1.840                       | 0.9971 |

$q_{e,\text{exp}} = q_{e,\text{experiment}}$

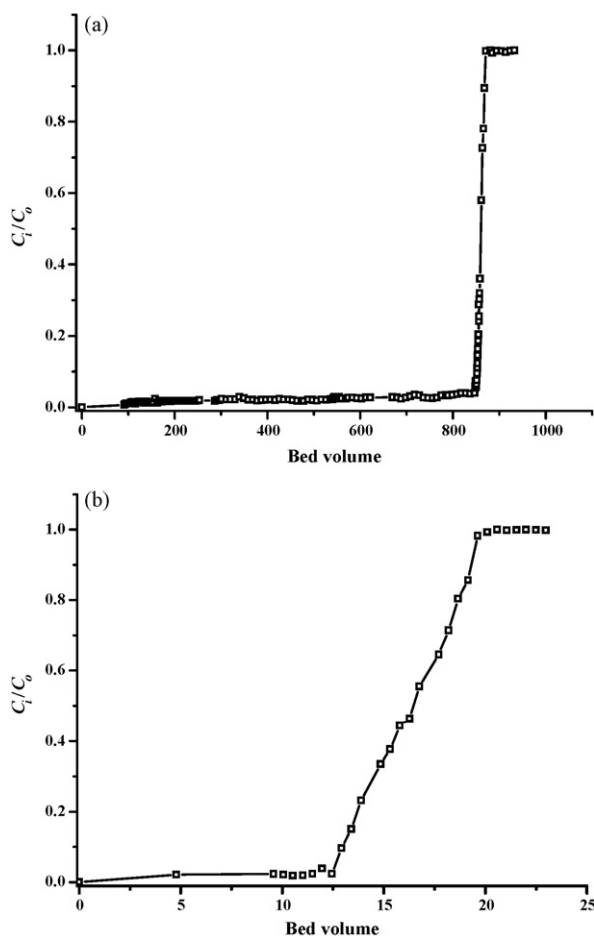


Fig. 4. (a) Breakthrough curve of phosphate in industrial wastewater on SSW-Fe column. (b) Breakthrough curve of phosphate in industrial wastewater on SSW-Al column.

In addition, the sharp breakthrough curves indicate the excellent availability of the columns.

In order to describe the adsorption process of phosphate in the columns, the Yoon and Nelson model (4) was adopted to fit the adsorption breakthrough curves. The Yoon and Nelson model is widely applied to a single component system, and expressed as [25]:

$$\ln \left[ \frac{C_t}{(C_i - C_t)} \right] = K_{YN}(t - \theta) \quad (4)$$

where  $C_i$  and  $C_t$  are the concentrations of phosphate (mg/L) in influent and at time ( $t$ ) in effluent, respectively,  $t$  is the service time of the column (h),  $K_{YN}$  is proportionality constant ( $\text{min}^{-1}$ ) and  $\theta$  (h) is the breakthrough time when  $C_t/C_i$  equals 0.5. The calculated parameters of Yoon and Nelson model ( $K_{YN}$  and  $\theta$ ) are presented in Table 5.

As summarized in Table 5, the values of  $\theta$  calculated from the model are in agreement with the ones obtained from column experiments, which confirms the applicability of Yoon and Nelson model to this single component column system. However, the applicabil-

Table 5  
The Yoon–Nelson model parameters obtained from the fitting of breakthrough curves.

| Material | $K_{YN}$ ( $\text{h}^{-1}$ ) | $\theta$ (h) | $\theta_{\text{exp}}$ (h) | $R^2$  |
|----------|------------------------------|--------------|---------------------------|--------|
| SSW-Fe   | 0.4856                       | 448.5        | 449.6                     | 0.9799 |
| SSW-Al   | 1.360                        | 8.561        | 8.750                     | 0.9342 |

Table 6  
Concentrations of leached ions in effluent of column adsorption.

| Sampling point (mL) | Concentration of leached metal ions |                    |
|---------------------|-------------------------------------|--------------------|
|                     | Fe (mg/L) (SSW-Fe)                  | Al (mg/L) (SSW-Al) |
| 100                 | 0                                   | 0.005              |
| 200                 | 0                                   | 0.002              |
| 300                 | 0                                   | 0.003              |
| 400                 | 0                                   | 0.003              |
| 1000                | 0.005                               | –                  |
| 2000                | 0.023                               | –                  |
| 5000                | 0.026                               | –                  |
| 10000               | 0.062                               | –                  |
| 15000               | 0.059                               | –                  |
| 18000               | 0.050                               | –                  |

–: No metal ion was detected.

ity of Yoon and Nelson model in industrial scale should be further investigated. Another simple model (5) suggested by Chen [26] was employed to calculate the adsorption capacity of SSW-Fe or SSW-Al column to phosphate.

$$X = \frac{\left( t_e - \int_{t_b}^{t_e} f(t) dt \right) Q C_i}{W} \quad (5)$$

where  $Q$ ,  $C_i$  and  $W$  are volumetric flow rate (mL/min), influent concentration (mg/L) and weight of adsorbent (g);  $t_e - \int_{t_b}^{t_e} f(t) dt$  is the area under the breakthrough curve which can be calculated through integration;  $t_b$ ,  $t_e$  and  $f(t)$  are the function parameters representing the time of breakthrough point ( $t_b$ ), time at exhaustion ( $t_e$ ) and effluent profile, respectively. Calculated by Eq. (5), the adsorption capacities of SSW-Fe and SSW-Al are 7.28 mg P/g and 0.166 mg P/g, respectively, which are consistent with the results obtained from column experiments, but much lower than those obtained from batch experiments.

It is necessary to point out that the adsorption conditions of column system and batch experiment are very different. The column adsorption is a dynamic process and the adsorption proceeds in an unstable state. The influent continuously meets a fresh part of adsorbent when it passes through the column and trends to establish a new equilibrium of adsorption. However, a true equilibrium is never attained, because the contact time in column system is limited [27]. In column experiments, the average contact time of SSW-Fe or SSW-Al can be calculated as:

$$t_c = \frac{V}{Q} \quad (6)$$

where  $t_c$  is the average contact time (min),  $V$  and  $Q$  are column volume (mL) and flow rate (mL/min) of phosphate wastewater, respectively. Calculated by Eq. (6), the average contact times of phosphorous industrial wastewater in SSW-Fe and SSW-Al columns are both 30 min. According to the adsorption kinetics investigation in Section 3.2, approximately 50% of adsorption equilibrium was attained in column. The limited contact time greatly decreases the adsorption capacity of adsorbents. Therefore, the adsorption capacity in column adsorption is lower than that in batch adsorption.

### 3.4. Stability of adsorbents

In consideration of practical application, adsorbent should be stable during operation process. It can be seen from Table 2, the denaturation temperatures of SSW-Al and SSW-Fe are high enough to satisfy the demand of practical application. Furthermore, the concentration of leaked Fe(III) or Al(III) ion in the effluent of column adsorption is neglectable, as shown in Table 6. These facts indicate that SSW-Fe and SSW-Al are stable adsorbents when used for removal of phosphate from industrial wastewater.

#### 4. Conclusions

Fe(III)- and Al(III)-loaded adsorbents can be prepared by using skin split waste of tannery as supporting matrix. As expected, these adsorbents, especially SSW-Fe, exhibit high adsorption capacity to phosphate. The adsorption rate of phosphate on the adsorbents can be well described by the pseudo-second-order model, due to the fact that the adsorbents are in fibrous state and thus the diffusion resistance of mass transfer is neglectable. Based on the column adsorption experiments, it can be concluded that the phosphate in industrial wastewater can be efficiently removed by these adsorbents. So this research suggests that the skin split waste in tannery can be transformed into low cost and environment protection material.

#### Acknowledgements

We acknowledge the financial supports provided by National Technologies R&D Program (2006BAC02A09), Sichuan Province Technologies R&D Program (2008GZ0026) and The Key Program of National Science Fund of China (20536030).

#### References

- [1] P.S. Lau, N.F.Y. Tam, Y.S. Wong, Wastewater nutrients (N and P) removal by carrageenan and alginate immobilized *Chlorella vulgaris*, *Environ. Technol.* 18 (1997) 945–951.
- [2] C.Y. Wang, J.P. Zhai, R. Nie, L. Huang, Experimental study on phosphorus removal by activated sludge process in treating wastewater of low phosphorus concentration, *Environmental Protection Science* 31 (4–6) (2005) 20 (in Chinese).
- [3] L.E. de-Bashan, Y. Bashan, Recent advances in removing phosphorus from wastewater and its future use as fertilizer (1997–2003), *Water Res.* 38 (2004) 4222–4246.
- [4] E. Yildiz, Phosphate removal from water by fly ash using crossflow microfiltration, *Sep. Purif. Technol.* 35 (2004) 241–252.
- [5] K. Fytianos, E. Voudrias, N. Raikos, Modelling of phosphorus removal from aqueous and wastewater samples using ferric iron, *Environ. Pollut.* 101 (1998) 123–130.
- [6] S.H. Lee, B.C. Lee, K.W. Lee, S.H. Lee, Y.S. Choi, K.Y. Park, M. Iwamoto, Phosphorus recovery by mesoporous structure material from wastewater, *Water Sci. Technol.* 55 (2007) 169–176.
- [7] L. Johansson, J.P. Gustafsson, Phosphate removal using blast furnace slags and opoka-mechanisms, *Water Res.* 34 (2000) 259–265.
- [8] Y. Yang, D. Tomlinson, S. Kennedy, Y.Q. Zhao, Dewatered alum sludge: a potential adsorbent for phosphorus removal, *Water Sci. Technol.* 54 (2006) 207–213.
- [9] Y.Z. Li, C.J. Liu, Z.K. Luan, X.J. Peng, C.L. Zhu, Z.Y. Chen, Z.G. Zhang, J.H. Fan, Z.P. Jia, Phosphate removal from aqueous solutions using raw and activated red mud and fly ash, *J. Hazard. Mater.* 137 (2006) 374–383.
- [10] C. Namasivayam, K. Prathap, Recycling Fe(III)/Cr(III) hydroxide, an industrial solid waste for the removal of phosphate from water, *J. Hazard. Mater.* 123 (2005) 127–134.
- [11] Z.K. Zhang, G.Y. Li, B. Shi, Physicochemical properties of collagen, gelatin and collagen hydrolysate derived from bovine limed split wastes, *J. Soc. Leather Technol. Chem.* 90 (2006) 23–28.
- [12] B.O. Bitlishi, E. Karacaki, Utilization of leather industry solid wastes in the production of porous clay brick, *J. Soc. Leather Technol. Chem.* 90 (2006) 19–22.
- [13] A.R. El Boushy, A.F.B. van der Poel, J.I.A. Koene, S.H. Dieleman, Tanning waste by-product from cattle hides, its suitability as a feedstuff, *Bioresource Technol.* 35 (1991) 321–323.
- [14] L.S. Simeonova, P.G. Dalev, Utilization of a leather industry waste, *Waste Manage.* 16 (1996) 765–769.
- [15] J.A. Munoz, A. Gonzalo, M. Valiente, Arsenic adsorption by Fe(III)-loaded open-celled cellulose sponge. Thermodynamic and selectivity aspects, *Environ. Sci. Technol.* 36 (2002) 3405–3411.
- [16] H.S. Altundogan, F. Tumen, Removal of phosphate from aqueous solutions by using bauxite. I. Effect of pH on the adsorption of various phosphates, *J. Chem. Technol. Biotechnol.* 77 (2001) 77–85.
- [17] X.P. Liao, Y. Ding, B. Wang, B. Shi, Adsorption behavior of phosphate on metal-ions-loaded collagen fiber, *Ind. Eng. Chem. Res.* 45 (2006) 3896–3901.
- [18] C. Namasivayam, D. Sangeetha, Equilibrium and kinetic studies of adsorption of phosphate onto ZnCl<sub>2</sub> activated coir pith carbon, *J. Colloid Interface Sci.* 280 (2004) 359–365.
- [19] P. Ning, C.L. Deng, H.P. Pu, L.M. Niu, Adsorption of phosphate from water with active alumina nonferrous metals, *Nonferrous Metals* 54 (2002) 37–39 (in Chinese).
- [20] S. Tanada, M. Kabayama, N. Kawasaki, T. Sakiyama, T. Nakamura, M. Araki, T. Tamura, Removal of phosphate by aluminum oxide hydroxide, *J. Colloid Interface Sci.* 257 (2003) 135–140.
- [21] I. Langmuir, The constitution and fundamental properties of solids and liquids, *J. Am. Chem. Soc.* 38 (1916) 2221–2295.
- [22] H.M.F. Freundlich, Tiber die adsorption in losungen, *Z. Phys. Chem.* 57 (1906) 385–470.
- [23] E. Ou, Z.J. Junjie, M.C. Shaochun, W.Q. Jiaqiang, X. Fei, M. Liang, Highly efficient removal of phosphate by lanthanum-doped mesoporous SiO<sub>2</sub>, *Colloids Surf. A: Physicochem. Eng. Aspects* 308 (2007) 47–53.
- [24] V. Lenoble, O. Bouras, V. Deluchat, B. Serpaud, J.C. Bollinger, Arsenic adsorption onto pillared clays and iron oxides, *J. Colloid Interface Sci.* 255 (2002) 52–58.
- [25] Y.H. Yoon, J.H. Nelson, Application of gas adsorption kinetics. I. A theoretical model for respirator cartridge service life, *Am. Ind. Hyg. Assoc. J.* 45 (1984) 509–516.
- [26] J.P. Chen, J.T. Yoon, S. Yiacoumi, Effects of chemical and physical properties of influent on copper sorption onto activated carbon fixed-bed columns, *Carbon* 41 (2003) 1635–1644.
- [27] A.A. Attia, B.S. Girgis, N.A. Fathy, Removal of methylene blue by carbons derived from peach stones by H<sub>3</sub>PO<sub>4</sub> activation: Batch and column studies, *Dyes Pigments* 76 (2008) 282–289.